Correlation between Exchange Bias and Pinned Interfacial Spins

H. Ohldag,[1,2,3,*] A. Scholl,[2] F. Nolting,[4] E. Arenholz,[2] S. Maat,[5] A. T. Young,[2] M. Carey,[5] and J. Stöhr[1]

[1]*Stanford Synchrotron Radiation Laboratory, P.O. Box 20450, Stanford, California 94309, USA*

[2]*Advanced Light Source, One Cyclotron Road, Lawrence Berkeley National Laboratory, Berkeley, California 94720, USA*

[3]*Institut für Angewandte Physik, Universität Düsseldorf, 40225 Düsseldorf, Germany*

[4]*Swiss Light Source, Paul Scherrer Institut, CH-5232 Villigen PSI, Switzerland*

[5]*Hitachi Global Storage Technologies, San Jose Research Center, 650 Harry Road, San Jose, California 95120, USA*

(Received 19 October 2002; published 1 July 2003)

Using x-ray magnetic circular dichroism, we have detected the very interfacial spins that are responsible for the horizontal loop shift in three different exchange bias sandwiches, chosen because of their potential for device applications. The "pinned" uncompensated interfacial spins constitute only a fraction of a monolayer and do not rotate in an external magnetic field since they are tightly locked to the antiferromagnetic lattice. A simple extension of the Meiklejohn and Bean model is proposed to account quantitatively for the exchange bias fields in the three studied systems from the experimentally determined number of pinned moments and their sizes.

DOI: 10.1103/PhysRevLett.91.017203 PACS numbers: 75.70.Rf, 75.50.Ee, 78.20.Ls

Many of today's advanced magnetic devices, such as spin valves for magnetic recording read heads [1], rely on an effect called exchange bias, where the magnetization of a ferromagnetic layer is pinned into a well-defined reference direction by an antiferromagnet such that its hysteresis loop exhibits a *horizontal* shift [2,3]. Extensive research has led to the notion that the exchange bias effect must originate from uncompensated interfacial spins that are anchored in the antiferromagnet (i.e., are *pinned*) and do not follow the external field (for a review, see [4,5]). Today, the detection of the pinned spins, the determination of their origin and size, and their quantitative link to the size of the bias effect remain forefront research problems.

Uncompensated spins associated with antiferromagnets or their interfaces have been observed in several systems, such as CoO/MgO [6] using SQUID or Co/FeMn [7], Co/IrMn [8], and Co/NiO [9] using x-ray magnetic circular dichroism (XMCD). In particular, the study of Co/NiO showed that the existence of uncompensated interfacial spins is insufficient for exchange bias since they may more strongly couple to and rotate with the ferromagnet, yielding no bias. Experimental evidence for pinned spins has been reported only for single-crystal-like Fe/FeF_2 and Fe/MnF_2 where a perpendicular coupling between the spin axes of the ferromagnet (FM) and antiferromagnet (AFM) has been suggested [10]. Hysteresis loops obtained from these samples also exhibited a vertical loop shift indicating the presence of pinned spins in the sample. However, the exact location of the pinned spins could not be specified. Hence, a quantitative correlation between the experimentally determined pinned magnetization and the macroscopic exchange bias field, crucial to the microscopic understanding of exchange bias, has not been achieved thus far.

Here we present results for three polycrystalline exchange bias sandwiches, NiO/Co, IrMn/Co, and $PtMn/Co_{90}Fe_{10}$, chosen for their technological relevance and prototypical behavior. We used high sensitivity XMCD spectroscopy in total electron yield (TEY) detection to identify uncompensated Ni or Mn spins, located at the respective AFM-FM interfaces [9]. The TEY method offers sensitivity to the interfacial region because of the limited $1/e$ probing depth, as explained in detail previously [9,11]. By measurement of the Ni or Mn XMCD hysteresis loops, we show that only a small fraction of the interfacial spins, about 4% of a monolayer (ML), is tightly pinned to the AFM and does not rotate in an external field. The size of the pinned interfacial magnetization is found to be *quantitatively* correlated to the macroscopic magnetic exchange bias field, using a modified simple model, originally suggested by Meiklejohn and Bean [2,3].

All samples, Co(3 nm)/NiO(50 nm), $Co(2\text{ nm})/Ir_{20}Mn_{80}(20\text{ nm})$/Cu(2.5 nm)/Ta(5 nm), and $Co_{90}Fe_{10}(t\text{ nm})$/PtMn(25 nm)/Ta(5 nm), with $t = 1$ nm, 2 nm, and 3 nm, were grown at Hitachi by dc magnetron sputtering on Si wafers at room temperature under an Ar pressure of 2 mTorr. The NiO layer, in particular, was reactively sputtered from a Ni target under a partial oxygen pressure of 0.2 mTorr. To introduce exchange biasing, the Co/NiO and $Co_{90}Fe_{10}$/PtMn samples were *field annealed* in a 1 Tesla field. The PtMn samples were annealed at 525 K for 4 h, while the Co/NiO sample was annealed at 470 K for 1 h. In contrast, one of the $Co/Ir_{20}Mn_{80}$ samples was exchange biased by deposition in an applied magnetic field of 50 Oe (*field grown*), while the second one was prepared without an applied field (*zero-field grown*) for reference purposes. All samples were protected with thin (~ 2 nm) coatings (Pd, Pt, or Ru) against oxidation. In all cases, the remanent magnetization direction (easy axis) was in the plane of the sample.

X-ray absorption spectra were obtained by recording the sample current as a function of x-ray energy. We used

left and right elliptically polarized x rays with a degree of circular polarization $p = \pm 0.81$ from an elliptical polarized undulator on beam line 4.0.2 at the Advanced Light Source [12]. The x rays were incident at a grazing angle of 30° from the sample surface, either parallel or antiparallel to the bias direction. Magnetic fields of up to ± 0.28 T were applied along the x-ray propagation direction using an electromagnet.

First, the total coverage with uncompensated spins at the interface is determined. Figures 1(a) and 1(b) show absorption spectra measured on Co/IrMn and Co/NiO, that were acquired for two opposite sample magnetization directions (red and blue) relative to the fixed helicity of the elliptically polarized x rays. The difference spectra (below) demonstrate a magnetic circular dichroism at the Co L_3 and L_2 edges. In addition, uncompensated and rotatable Ni or Mn spins which follow the ferromagnetic Co spins near the surface of the antiferromagnet lead to a weak but still clearly visible ferromagnetic signal. For both systems, it exhibits the same sign as the Co signal, demonstrating that the coupling between the magnetization of the FM and the AFM is parallel or ferromagnetic. From the size of the dichroism, we estimate a nominal thickness of the rotatable magnetization of (0.44 ± 0.11) ML for Co/NiO and (0.52 ± 0.13) ML for $Co/Ir_{20}Mn_{80}$ [13].

In order to determine whether all the observed interfacial spins are rotatable, element specific hysteresis loops $\vec{M}(\vec{H})$ were recorded. For clarity, the effect of a pinned magnetization onto the shape of the hysteresis loop is illustrated in Fig. 2. On top, we show the two experimental geometries in which hysteresis loops were acquired, and the corresponding color-coded loops are shown below. The two loops describe a sample that contains rotating moments M_{rot} and a smaller number of pinned moments M_{pin}. The height of each loop corresponds to twice the rotating magnetization M_{rot}. The loops exhibit opposite horizontal and vertical shifts due to the reversal of the bias field direction relative to the applied field direction when the sample is rotated about a vertical axis. The vertical shift M_{pin} is due to pinned moments that are not rotated by the applied field and therefore define the bias direction. From the asymmetry between vertical loop shift and loop height, the ratio between pinned and rotating magnetization can be determined.

Four hysteresis loops were acquired by monitoring the sample current $I_n^p(\vec{H})$ as a function of the magnetic field $\vec{H}$ with the photon energy tuned to either of the L_n ($n = 2, 3$) resonances and using left and right elliptically polarized x rays ($p = \pm 0.81$). The monitored current for each loop is a superposition of the XMCD signal, nonmagnetic background in the absorption signal, and a modulation of the electron yield due to $\vec{H}$-field dependent deflection of the emitted electrons in the magnetic field. While the sample magnetization contributes with opposite sign to the asymmetry at the L_3 and L_2 edges, field-dependent artifacts contribute with the same sign. To cancel out these artifacts, we used the four experimental loops to first calculate asymmetry ratios between loops obtained with opposite helicity of the x rays

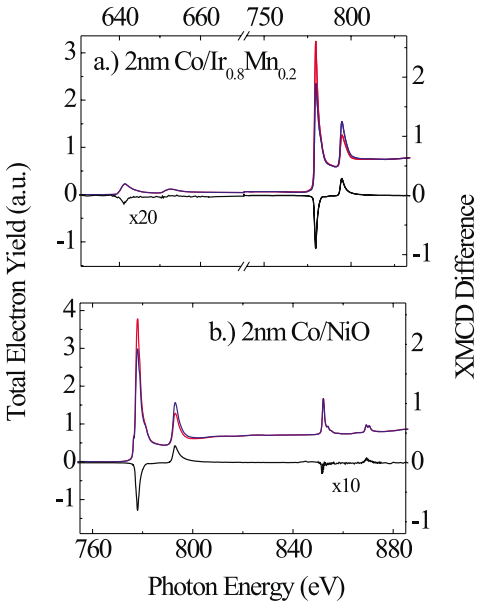

FIG. 1 (color). XMCD spectra of (a) Co(2 nm)/$Ir_{20}Mn_{80}$(20 nm) and (b) Co(3 nm)/NiO(50 nm). Shown are spectra for parallel (red) and antiparallel (blue) alignment of external field and x-ray helicity as well as their difference (black). Uncompensated and rotatable spins in the antiferromagnet are responsible for the observed Mn and Ni dichroism.

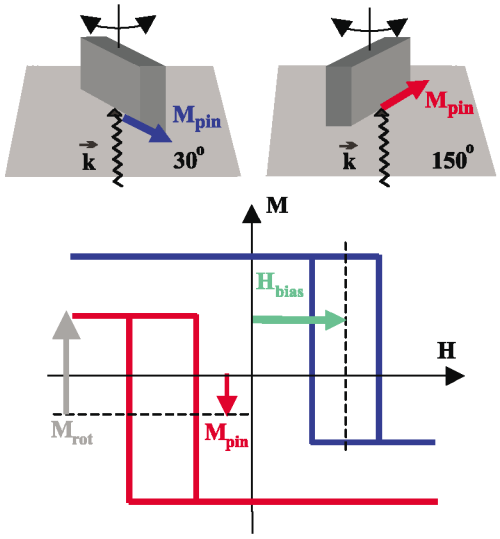

FIG. 2 (color). Top: Experimental geometry used for the acquisition of the XMCD hysteresis loops. The $\vec{H}$ field is along the x-ray wave vector $\vec{k}$. The angle between exchange bias field and incident x rays was varied between 30° (blue) and 150° (red). Bottom: Schematic hysteresis loops in the presence of rotating and pinned moments in an exchange biased sample. The arrows refer to the rotating magnetization (gray), the pinned magnetization (red), and the bias field (green).

($p = \pm 81\%$) at either the L_3 or the L_2 energy position and then took the difference of the ratios [14]. For the final results, up to 20 loops were typically averaged with an acquisition time of 15 min per loop.

The experimental loops obtained from Co and Mn in field deposited (left) and zero-field deposited (right) $Co/Ir_{20}Mn_{80}$ in the two different experimental geometries are shown in Fig. 3. We note upfront that corresponding data acquired on bare $Ir_{20}Mn_{80}$ films and normalized identically did not show any magnetic hysteresis and would simply yield a horizontal line at zero magnetization in Fig. 3. Also, because of the small size of the measured Mn signal, we carefully checked the consistency of the measured shifts and normalization by an additional azimuthal rotation of the samples about the surface normal. The hysteresis loops acquired on the field deposited sample exhibit a rectangular shape and a horizontal shift of 570 Oe. In contrast, the loops obtained from the zero-field deposited sample do not indicate the presence of a macroscopic uniaxial or unidirectional anisotropy. This is similar to the case of an exchange coupled sample, which has been ac demagnetized during field cooling [16]. Here, due to the absence of a magnetic field during growth, no orientation of the as-deposited antiferromagnetic $Ir_{20}Mn_{80}$ layer is achieved and, hence, an isotropic magnetic behavior is observed overall [17].

Both the Co spins in the FM and the Mn spins in the AFM exhibit identical coercivities and bias fields and also reveal an overall similar shape. In addition, the Mn loops of the field deposited sample exhibit a small vertical offset that is absent in the Mn loops of the zero-field deposited sample. The vertical offset in the Mn loops—as explained in Fig. 2—indicates that in the biased sample a small fraction of about $(7 \pm 2)\%$ of the total uncompensated moments of 0.56 ± 0.14 ML is pinned, yielding a pinned coverage $\rho = (0.04 \pm 0.01)$ ML. On the other hand, the majority of uncompensated Mn moments rotates with the ferromagnetic Co. Similar results were obtained for Co/NiO and $Co_{90}Fe_{10}$/PtMn. The interface coupling in all three studied systems is parallel, and in all cases the thickness of the pinned magnetization was determined to lie in the range 0.03–0.04 monolayers (see Table I). No vertical shift was detected in any of the Co loops. Since the major part of the Co XMCD signal originates from the bulk of the film, the absence of a vertical shift in the Co loop excludes the presence of pinned moments throughout the entire 2 nm thick Co film. The presence of a 0.04 ML thick layer of pinned Co spins only at the interface to the IrMn cannot be excluded since it will only lead to a vertical loop shift of 0.3%, which is too small to be detected.

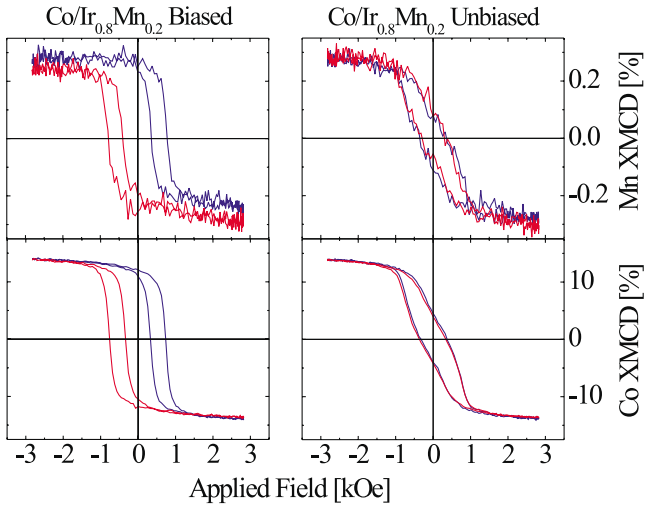

FIG. 3 (color). Element specific XMCD hysteresis loops $\vec{M}(\vec{H})$ measured on Co and Mn in Co(2 nm)/$Ir_{20}Mn_{80}$(50 nm). Loops of the field deposited sample are shown on the left while those from the zero-field deposited sample are shown on the right. The hysteresis loops were acquired with the bias field (horizontal loop shift) either parallel (red) or antiparallel (blue) to the propagation direction of the incident x rays.

The amount of pinned interfacial magnetization is correlated to the observed macroscopic bias fields following the original idea of Meiklejohn and Bean [2,3]. The macroscopic bias field $\vec{H}_B$ of an epitaxial, fully uncompensated and pinned ferromagnet/antiferromagnet interface can be written as a function of the unidirectional magnetic interface energy σ and the Heisenberg-like interface exchange energy J, according to

$$H_B = \frac{\sigma}{M_{\mathrm{FM}} t_{\mathrm{FM}}} = J \frac{S_{\mathrm{AFM}} S_{\mathrm{FM}}}{a_{\mathrm{AFM}}^2 M_{\mathrm{FM}} t_{\mathrm{FM}}}. \quad (1)$$

M_{FM} and t_{FM} are the magnetization and the thickness of the FM, a_{AFM} is the size of the unit cell of the AFM, and S_{FM} and S_{AFM} are the atomic magnetic moments of the FM and the AFM. This model is applicable for artificial antiferromagnet/ferromagnet multilayer structures as shown by Jiang *et al.* [18], yet fails in nonideal systems, overestimating the interface coupling strength by orders of magnitude. Taking into account that only a small, pinned fraction ρ of the uncompensated interfacial moments contributes to bias, the ideal coupling energy J and, hence, the interfacial energy density σ can be substituted by effective values J_{eff} and σ_{eff}, which are defined in the following:

TABLE I. Effective and corrected interface energies σ calculated from the macroscopic loop shift and the coverage with pinned spins ρ.

	Sample	ρ (ML)	σ_{eff} (mJ/m^2)	σ (mJ/m^2)
A	3 nm Co/NiO	0.04 ± 0.01	0.052 ± 0.005	1.3 ± 0.5
B	2 nm Co/IrMn	0.04 ± 0.01	0.168 ± 0.020	4.1 ± 1.4
C	1 nm CoFe/PtMn	0.03 ± 0.01	0.124 ± 0.014	3.9 ± 1.4
D	2 nm CoFe/PtMn	0.04 ± 0.01	0.188 ± 0.015	4.8 ± 1.7
E	3 nm CoFe/PtMn	0.04 ± 0.01	0.229 ± 0.027	5.7 ± 2.0

$$\sigma_{\text{eff}} = \rho\sigma, \qquad J_{\text{eff}} = \rho J. \tag{2}$$

The results for different materials and FM thicknesses are tabulated in Table I. We list the nominal thickness ρ of the pinned uncompensated layer in fractions of a monolayer and the effective interface energy σ_{eff} calculated from the macroscopic exchange bias field. In agreement with numerous earlier studies [4,5], we obtain laterally averaged interface coupling energies σ_{eff}, which are about 2 orders of magnitude smaller than those expected for a fully uncompensated interface. This reduction is readily explained by the observed dilution of pinned uncompensated interface spins which can be used to renormalize the effective interface energy for the proper interface area leading to corrected interface energies σ between 1 and 6 mJ/m^2. These values are close in size to the predicted interface energies of an ideal, uncompensated interface of about 10 mJ/m^2 [4,5,19].

The values obtained for σ for the three different PtMn samples (C, D, and E) suggest that σ increases with the thickness of the ferromagnetic layer. This behavior is observed because we assume in Eq. (1) that the exchange bias field is inversely proportional to the thickness of the ferromagnetic layer. Other studies have shown that this dependence is strict only above a certain minimum thickness of the ferromagnet (for a reference, see [4]), which depends on the material and is typically a few nanometer. Below this thickness, lower values for H_B are observed as predicted by Eq. (1). Since the ferromagnetic films investigated here are close to the minimum thickness, the results are affected by this deviation and therefore σ is underestimated. Exchange biased samples with thicker ferromagnetic layers cannot be investigated by our method because of the limited probing depth of the TEY approach.

In summary, we have observed pinned uncompensated spins at the interface of several exchange bias sandwiches that are used in room temperature device structures. In all cases, we find that only 4% of the interface layer contains pinned spins. We believe that the tiny fraction of uncompensated pinned spins is the very reason that has impeded the unravelling of the exchange bias puzzle for nearly 50 years. We find that the size of the exchange bias field can be understood in terms of a simple extension of the early Meiklejohn and Bean model, which quantitatively explains the determined bias fields by the number of pinned interfacial moments and their size. It appears that the development of a domain wall parallel to the surface, either extending into the FM or the AFM [21–24], is not required, although its existence cannot be excluded. However, contributions to the unidirectional anisotropy energy from deeper layers in the antiferromagnet appear to be small relative to contributions originating from pinned spins in close proximity to the interface, which are detected by our method. The origin of the pinned spins still evades us, but it is tempting to speculate from their approximately constant number in the different samples (see Table I) and from the typical crystallographic grain size of 20 nm in our polycrystalline films [25] that they are located at grain (= domain) boundaries, since these cover about the same percentage of the interface.

*Author to whom correspondence should be addressed. Electronic address: hohldag@stanford.edu

[1] B. Dieny *et al.*, Phys. Rev. B **43**, 1279 (1991).
[2] W. H. Meiklejohn and C. P. Bean, Phys. Rev. **102**, 1413 (1956).
[3] W. H. Meiklejohn, J. Appl. Phys. **33**, 1328 (1962).
[4] J. Nogués and I. K. Schuller, J. Magn. Magn. Mater. **192**, 203 (1999).
[5] A. E. Berkowitz and K. Takano, J. Magn. Magn. Mater. **200**, 552 (1999).
[6] K. Takano *et al.*, Phys. Rev. Lett. **79**, 1130 (1997).
[7] W. J. Antel, F. Perjeru, and G. R. Harp, Phys. Rev. Lett. **83**, 1439 (1999).
[8] T. P. A. Hase *et al.*, Appl. Phys. Lett. **79**, 985 (2001).
[9] H. Ohldag *et al.*, Phys. Rev. Lett. **87**, 247201 (2001).
[10] J. Nogués, C. Leighton, and I. K. Schuller, Phys. Rev. B **61**, 1315 (2000).
[11] T. Regan *et al.*, Phys. Rev. B **64**, 214422 (2001).
[12] A. T. Young *et al.*, Nucl. Instrum. Methods Phys. Res., Sect. A **467**, 549 (2001).
[13] For this analysis, we use the atomic moment of the ferromagnet and assume that all uncompensated spins are located at the interface. For IrMn, we assume a magnetic moment of $3.4\mu B$, for PtMn $4.2\mu B$, and for Ni $2.0\mu B$. The error bars result from the error with which the XMCD asymmetry can be determined (10%) and the error which we allow for the magnetic moment (20%).
[14] Altogether, the resulting loop $\vec{M}(\vec{H})$ can be written as $(I_3^+ - I_3^-)/(I_3^+ + I_3^-) - (I_2^+ - I_2^-)/(I_2^+ + I_2^-)$; for a similar approach see Goering *et al.* [15]
[15] E. Goering *et al.*, J. Appl. Phys. **88**, 5920 (2000).
[16] N. J. Gökemeijer, J. W. Cai, and C. L. Chien, Phys. Rev. B **60**, 3033 (1999).
[17] F. Nolting *et al.*, Nature (London) **405**, 767 (2000).
[18] J. S. Jiang *et al.*, Phys. Rev. B **61**, 9653 (2000).
[19] Furthermore, reasonable Heisenberg exchange constants of 1–7 meV [20] can be obtained by multiplying the corrected interface energy densities σ with a typical antiferromagnetic unit cell area of 0.15 nm^2.
[20] M. Pajda *et al.*, Phys. Rev. B **64**, 174402 (2001).
[21] M. D. Stiles and R. D. McMichael, Phys. Rev. B **59**, 3722 (1999).
[22] D. Mauri, H. Siegmann, P. Bagus, and E. Kay, J. Appl. Phys. **62**, 3047 (1987).
[23] M. Kiwi, J. Mejia-López, R. D. Portugal, and R. Ramírez, Appl. Phys. Lett. **75**, 3995 (1999).
[24] P. Miltényi *et al.*, Phys. Rev. Lett. **84**, 4224 (2000).
[25] The grain size of samples grown under the conditions described above has been determined by x-ray diffraction (IrMn/PtMn) or atomic force microscopy (NiO).